Supplementary Note

Physical Model of Cell Shapes in the Mouse Embryo

1 General framework

We describe here a theory predicting the shape of blastomeres in the pre-implentation mouse embryo. This model is an extension of our previous approach used to study compaction at the 8-cell stage[1]. The shape of cells, their contacts and the overall arrangement of the cells in space are controlled by effective surface tensions associated to the different interfaces found between cells, and between a cell and the surrounding medium. We suppose here that all cell-cell interfaces have the same tension, but that tensions at cell-medium interfaces can be different. We note γ_i the surface-tension at the cell-medium interface of a given cell i, and γ_c the surface tension at cell-cell interfaces. Moreover, we assume that each blastomere conserves its volume at any time, as previously verified[1].

Because cell internalization in the 16-cell stage mouse embryo (or in doublets of 16-cell stage blastomeres) happens on hours timescales, we can neglect mechanical dissipation, which have a typical timescale of the order of minutes[2]. This corresponds to a quasistatic regime, in which blastomeres always have enough time to reach static mechanical equilibrium, such that the evolution of their shape is controlled solely by slow changes in surface tensions. Hence, the conservation of cell volumes together with the minimization of the total effective surface energy define the configuration of the embryo.

We first present a model with two cells, which can be formulated analytically because of its axial symmetry. We then extend the model to 3 dimensions using triangulated surfaces, and we minimize the effective energy numerically for 2 or 16 cells. To validate the numerical model, we compare its predictions for a cell doublet to the ones given by the analytical model.

2 Internalization model for a cell doublet

2.1 Force balance

We first consider two cells in contact. With two cells only, the equilibrium configuration should have an axis of symmetry, while this result does generally not hold for more cells. We use Laplace's force balance $p_i - p_0 = 2\frac{\gamma_i}{R_i}$ at a given

interface i to relate the pressure difference across the interface $p_i - p_0$, the surface tension γ_i and the radius of curvature R_i of the interface. For a quasistatic evolution, the pressure difference and surface tension being considered homogeneous, Laplace's law predicts that the curvature for each interface should be constant, but curvature may vary between interfaces, according to their respective tensions.

We consider therefore a doublet of cells made of spherical interfaces, with γ_1 and γ_2 the cell-medium surface tension of cells 1 and 2, and γ_c the cell-cell interface tension. Calling $\vec{\mathbf{e}_z}$ the axis of symmetry, the doublet geometry can be described by the longitudinal cross-section represented in Supplementary Note Fig. 1.

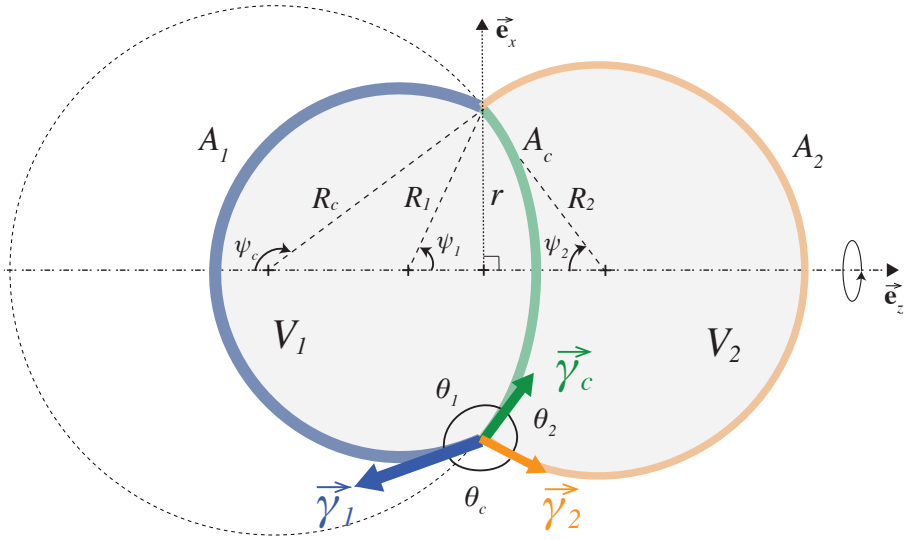

Supplementary Note Figure 1: Cross-section of the asymmetric cell doublet and parametrization of its shape. The cell-medium interface area, tension, curvature radius and volume of the cell $i = 1, 2$ are denoted respectively A_i, γ_i, R_i and V_i. The cell-cell contact tension and area are denoted respectively γ_c and A_c, and r denotes the radius of the contact line. We furthermore define the three contact angles θ_1, θ_2 and θ_c as in the main text, or use alternatively the angles ψ_1, ψ_2 and ψ_c.

The doublet shape can be parametrized by the interfaces curvature radii R_1, R_2 and R_c and the angles ψ_1, ψ_2 and ψ_c, as represented on Supplementary Note Fig. 1. These variables are linked by the geometric relation

$$R_1 \sin\psi_1 = R_2 \sin\psi_2 = R_c \sin\psi_c \tag{S1}$$

Laplace's force balance for the three interfaces reads

$$p_1 - p_0 = 2\frac{\gamma_1}{R_1}, \tag{S2a}$$

$$p_2 - p_0 = 2\frac{\gamma_2}{R_2}, \tag{S2b}$$

$$p_1 - p_2 = 2\frac{\gamma_c}{R_c} = 2\left(\frac{\gamma_1}{R_1} - \frac{\gamma_2}{R_2}\right). \tag{S2c}$$

Where p_1 and p_2 are the pressures inside the cells, and p_0 the pressure in the surrounding medium. Note that the actual value of p_0 does not affect the config-

uration of the cells, since only relative pressure differences matter in the force balance.

The force balance at the contact line reads

$$\overrightarrow{\gamma_1} + \overrightarrow{\gamma_2} + \overrightarrow{\gamma_c} = \overrightarrow{\mathbf{0}} \tag{S3}$$

where $\overrightarrow{\gamma_i}$ is the force vector corresponding to the surface tension $\gamma_i \equiv \left|\overrightarrow{\gamma_i}\right|$.

This vectorial relation can be projected respectively along $\overrightarrow{\mathbf{e}_z}$ and $\overrightarrow{\mathbf{e}_x}$ using the angles ψ_i

$$\gamma_1 \sin\psi_1 = \gamma_2 \sin\psi_2 + \gamma_c \sin\psi_c\,, \tag{S4a}$$
$$\gamma_1 \cos\psi_1 + \gamma_2 \cos\psi_2 + \gamma_c \cos\psi_c = 0\,. \tag{S4b}$$

Using the geometrical relations Eq. S8, we show that the force balance at the contact line projected on $\overrightarrow{\mathbf{e}_z}$ (Eq. S4a) is equivalent to the Laplace's force balance along the interface between the two cells Eq. S2c

$$\frac{\gamma_c}{R_c} = \frac{\gamma_1}{R_1} - \frac{\gamma_2}{R_2}$$

Note that one can alternatively use the natural contact angles θ_1, θ_2 and θ_c to write the force balance at the contact line. Projecting this balance along the directions parallel and perpendicular to $\overrightarrow{\gamma_c}$ yields

$$0 = \gamma_c + \gamma_1 \cos\theta_1 + \gamma_2 \cos\theta_2 \tag{S5a}$$
$$0 = \gamma_1 \sin\theta_1 + \gamma_2 \sin\theta_2 \tag{S5b}$$

This couple of equations Eq. S5 is equivalent to Eq. S4 by noting the following geometrical relation between the angles θ_i and ψ_i

$$\theta_c = \psi_1 + \psi_2 \tag{S6a}$$
$$\theta_1 = 2\pi - (\psi_1 + \psi_c) \tag{S6b}$$
$$\theta_2 = \psi_c - \psi_2 \tag{S6c}$$

Adding the two volume conservation constraints, given the volumes V_1 and V_2, and the doublet force balance, given the surface tensions γ_1, γ_2, and γ_c, the problem involves finally eight non-linear relations with an equal number of

unknowns ψ_1, ψ_2, ψ_c, R_1, R_2, R_c, p_1 and p_2:

$$R_1 \sin\psi_1 = R_c \sin\psi_c \tag{S7a}$$
$$R_2 \sin\psi_2 = R_c \sin\psi_c \tag{S7b}$$
$$0 = \gamma_1 \cos\psi_1 + \gamma_2 \cos\psi_2 + \gamma_c \cos\psi_c \tag{S7c}$$
$$\frac{\gamma_c}{R_c} = \frac{\gamma_1}{R_1} - \frac{\gamma_2}{R_2} \tag{S7d}$$
$$p_1 - p_0 = 2\frac{\gamma_1}{R_1} \tag{S7e}$$
$$p_2 - p_0 = 2\frac{\gamma_2}{R_2} \tag{S7f}$$
$$\mathscr{V}_1(\psi_1, R_1, \psi_c, R_c) = V_1 \tag{S7g}$$
$$\mathscr{V}_2(\psi_2, R_2, \psi_c, R_c) = V_2 \tag{S7h}$$

where the pressures $p_{1,2}$ shall be chosen to adjust the volumes $\mathscr{V}_{1,2}$ of the two cells, which can be calculated from the volume of a spherical cap of radius R and height h: $\frac{1}{3}\pi h^2(3R-h)$.

While the force balance problem above is well-posed, it can in fact be drastically simplified by reformulating it as the minimization of an effective surface energy, as shown below.

2.2 Surface energy approach

Re-parametrization

Using the geometrical relation

$$r = R_1 \sin\psi_1 = R_2 \sin\psi_2 = R_c \sin\psi_c \tag{S8}$$

where r denotes the radius of the circle at which the three interfaces meet, or contact line, we can re-parametrize the geometry using the radius r and the three lengths

$$a_1 = R_1 \cos\psi_1\,, \qquad a_2 = R_2 \cos\psi_2\,, \qquad a_c = R_c \cos\psi_c \tag{S9}$$

reducing therefore the number of geometric variables necessary to describe the doublet geometry from six to four (note that a_c is negative).

Volumes

The volume of each spherical cap can be expressed as

$$v_i = \frac{1}{3}\pi\left(R_i + a_i\right)^2\left(2R_i - a_i\right) = \frac{2}{3}\pi\left[\left(r^2 + a_i^2\right)^{3/2} + a_i^3 + \frac{3}{2}r^2 a_i\right] \tag{S10}$$

where $i \equiv 1, 2, c$ and the volumes of the two cells are then simply

$$\mathscr{V}_1 = v_1 + v_c\,, \qquad \mathscr{V}_2 = v_2 - v_c \tag{S11}$$

Areas

Similarly, the surface area of the interfaces are $A_i = 2\pi R_i(R_i + a_i) = 4\pi H(r, a_i)$, for $i \equiv 1, 2, c$, with:

$$H(r,a) = \frac{1}{2}\left[a^2 + r^2 + a\sqrt{a^2 + r^2}\right]. \tag{S12}$$

Non-dimensionalization of the problem

Without loss of generality, all lengths are normalized in the following by $R_0 \equiv \left(3V_2/4\pi\right)^{1/3}$, corresponding to a renormalization of volumes by V_2. This yields therefore $\overline{\mathscr{V}}_2 = 1$, and we define a dimensionless size asymmetry parameter β such that $\overline{\mathscr{V}}_1 = \beta^3$:

$$\beta \equiv \left(V_1/V_2\right)^{1/3} \tag{S13}$$

Cell 1 is smaller than cell 2 if $\beta \leq 1$, or the other way around if $\beta \geq 1$.

Surface energy potential

In a similar manner as Refs[1–3], we define a surface energy potential

$$E = \gamma_1 A_1 + \gamma_2 A_2 + \gamma_c A_c \tag{S14}$$

that we seek to minimize under the constraints $\overline{\mathscr{V}}_1 = \beta^3$ and $\overline{\mathscr{V}}_2 = 1$. The surface energy potential is non-dimensionalized by dividing it with by $4\pi\gamma_2$, which yields

$$\mathscr{E}\left(r, a_1, a_2, a_c\right) \equiv \frac{E}{4\pi\gamma_2} = \delta H(r, a_1) + H(r, a_2) + 2\alpha H(r, a_c) \tag{S15}$$

where we have defined two additional dimensionless parameters

$$\alpha = \frac{\gamma_c}{2\gamma_2}\,, \qquad \delta = \frac{\gamma_1}{\gamma_2} \tag{S16}$$

The first parameter $0 \leq \alpha \leq 1$ quantifies the degree of compaction of the doublet[1], whereas $\delta \geq 0$ measures the tension asymmetry between the two cells.

Mechanical equilibrium

To take into account of the volume constraints, we introduce the Lagrangian function:

$$\mathscr{L} = \mathscr{E} - \overline{p}_1\left(\overline{\mathscr{V}}_1(r, a_1, a_c) - \beta^3\right) - \overline{p}_2\left(\overline{\mathscr{V}}_2(r, a_2, a_c) - 1\right) \tag{S17}$$

where $\overline{p}_1$ and $\overline{p}_2$ are the two Lagrange multipliers, which can be interpreted as (renormalized) cell pressures with respect to the medium. Minimizing $\mathscr{E}$ under the two volumes constraints is then equivalent to finding a solution to the system of equations:

$$\frac{\partial \mathscr{L}}{\partial r} = \frac{\partial \mathscr{L}}{\partial a_1} = \frac{\partial \mathscr{L}}{\partial a_2} = \frac{\partial \mathscr{L}}{\partial a_c} = \frac{\partial \mathscr{L}}{\partial \overline{p}_1} = \frac{\partial \mathscr{L}}{\partial \overline{p}_2} = 0 \tag{S18}$$

The shape of the doublet is therefore fully determined by three dimensionless parameters: α, β and δ.

This gives six equations to solve, instead of eight previously. Note that the Lagrangian is not necessarily convex (or concave), and the optimum defined above is hence not necessarily an extremum. Optimizing the Lagrangian with respect to a_1 and a_2 leads to

$$\overline{p}_1 = \frac{\delta}{2\pi\sqrt{a_1^2 + r^2}}, \qquad \overline{p}_2 = \frac{1}{2\pi\sqrt{a_2^2 + r^2}} \tag{S19}$$

Note that by multiplying the renormalized pressures values above by the normalizing factor $4\pi\gamma_2$, we recover the Laplace force balance for the cell-medium interfaces of the two cells (Eq. S2), because $p_i - p_0 = 4\pi\gamma_2\,\overline{p}_i$ and $R_i = \sqrt{a_i^2 + r^2}$ for $i \equiv 1, 2$.

Replacing these normalized pressure values in the Lagrangian, the optimization with respect to p_1 and p_2 naturally enforces the volume constraints $\mathscr{V}_1 = \beta^3$ and $\mathscr{V}_2 = 1$, while the optimization with respect to a_c and r leads to the equations corresponding to the balance of forces at the contact line (Eq. S3).

Thus minimizing the surface energy potential Eq. S14 under the two constraints of volume conservation yields exactly the same mathematical result as the one defined previously by the balance of forces in the doublet.

2.3 Internalization threshold

We first note that for $V_1 = V_2$ and $\gamma_1 = \gamma_2$, the doublet is symmetric ($\beta = 1$ and $\delta = 1$) corresponding to the problem that was solved previously [1] with a single parameter α.

For the non-symmetric case, solutions are obtained numerically using Mathematica by solving the constrained minimization problem above for various values of α, β and δ. The results are presented in the main text Fig. 2 and as Extended Data Fig. 3, with two phase-diagrams illustrating the equilibrium

shape of cell doublets and the unique transition to complete internalization. We find numerically that the cell 1 is fully internalized by the cell 2 if, and only if, $\delta \geq 1+2\alpha$. This relation corresponds to $\gamma_1 \geq \gamma_2 + \gamma_c$.

We note that the internalization threshold, corresponding to $\delta_c = 1+2\alpha$ is consistent with previous numerical results, obtained in the context of 2-dimensional multi-cellular tissues[4,5] or of emulsions[6].

We predict furthermore that this internalization threshold does not depend on the volume asymmetry defined by β. Volume asymmetries nevertheless affect the doublet shape for tension asymmetries lower than the threshold. For instance, changing β for a doublet with symmetric tensions ($\delta = 1$ leads to a partial ingress of one cell into the other, because of the difference in Laplace's pressures between the two cells originating from their different curvature radii (see Extended Data Fig. 3). However, a volume asymmetry is never sufficient to get complete internalization as it does not affect the predicted internalization threshold δ_c.

3 3D numerical model

The symmetry of revolution that was used in the analytical model for a cell doublet does not hold in general for more than two cells. We have thus developed a 3-dimensional model, in which each cell is defined by a triangulated surface and can occupy an arbitrary volume, as illustrated on Supplementary Note Fig. 2. To handle multimaterial interfaces in three dimensions, our simulations are based on a custom-modified version of the mesh tracking method *Multitracker*[7]. The energy of the system is calculated given the coordinates of all vertices forming the triangles, and given the surface tensions for each interface. The identity of each interface separating the cells i and j is simply tracked over its evolution by a label (i, j) that is stored in each triangle of this interface. A gradient descent numerical optimization scheme is then used to evolve cells shape towards static mechanical equilibrium. To maintain numerical precision, the triangular mesh is furthermore allowed to vary the number of vertices, edges and faces over its evolution (remeshing), and to perform topological T1 and T2 transitions. Note that, in contrast to classical vertex models where cell-cell boundaries are assumed to remain flat[8], our 3-dimensional model does not impose any prior constraints on cell shapes, and its precision of smooth and continuous interfaces is only limited by the user-defined precision for the triangular mesh discretization .

Supplementary Note Figure 2: Non-manifold triangular mesh and labeling of cells 1 and 2.

3.1 Generalized surface energy potential

The surface energy potential defined for the doublet can be generalize to n cells as

$$E = \sum_{i=1}^{n} \gamma_i A_i + \gamma_c \sum_{i=1}^{n} \sum_{j=i+1}^{n} A_{ij} \tag{S20}$$

where A_i and γ_i are respectively the area and the tension of the interface between the medium and cell i, while A_{ij} and γ_c are the area and the tension of the interface between cells i and j. The energy is a function of the coordinates of all vertices in the system.

Moreover, we suppose that each cell conserves its volume during shape changes and we minimize the generalized surface energy under these constraints. The energy is minimized iteratively with respect to the state variables (the vertex coordinates) using a gradient descent method. For a vertex $\mathbf{v}$ the descent step is given by

$$d\mathbf{v} = -h \frac{\partial E}{\partial \mathbf{v}} \tag{S21}$$

To find the scalar parameter h that defines the amplitude of displacement (h is the same for all vertices), we use a line-search method at each descent step. The volume constraints are enforced using a fast force projection method[9]. Finally, we consider that the minimization process has converged when the relative variation in the mesh surface energy is lower than 10^{-9}, corresponding to the numerical precision of the machine.

To verify our numerical implementation, we compare the numerical results obtained with two cells, with the results of the analytical model for a cell doublet. As illustrated on Extended data Fig. 7, the results of the 3D simulations remain perfectly axisymmetric, and match quantitatively with the analytical theory.

References

1. Maître, J.-L., Niwayama, R., Turlier, H., Nédélec, F., Hiiragi, T. Pulsatile cell-autonomous contractility drives compaction in the mouse embryo. *Nat. Cell Biol.* **17**, 849–855 (2015)
2. Turlier, H., Audoly, B., Prost, J., Joanny, J.-F. Furrow Constriction in Animal Cell Cytokinesis. *Biophys. J.* **106**, 114–123 (2014).
3. Goel, N. S., Doggenweiler, C. F., Thompson, R. L. Simulation of cellular compaction and internalization in mammalian embryo development as driven by minimization of surface energy. *Bull. Math. Biol.* **48**, 167–187 (1985).
4. Graner, F. Can Surface Adhesion Drive Cell-rearrangement? Part I: Biological Cell-sorting. *J. Theo. Biol.* **164**, 455–476 (1992).
5. Brodland, G. W. The Differential Interfacial Tension Hypothesis (DITH): A Comprehensive Theory for the Self-Rearrangement of Embryonic Cells and Tissues. *J. Biomech. Eng.* **124**, 188–197 (2002).
6. Guzowski, J., Korczyk, P. M., Jakiela, S., Garstecki, P. The structure and stability of multiple micro-droplets. *Soft Matter* **8**, 7269–11 (2012).
7. Da, F., Batty, C., Grinspun, E. Multimaterial Mesh-Based Surface Tracking. *ACM Trans. Graph.* **33**, 112:1-11 (2014).
8. Fletcher, A.G., Osterfield, M., Baker, R.E., Shvartsman, S.Y. Vertex Models of Epithelial Morphogenesis. Biophys. J. **106**, 2291–2304 (2014).
9. Brakke, K. A. The Surface Evolver. *Exp. Math.* **1**, 141–165 (1992).